# Spectroscopic study of $Nd^{3+}$ ions in $0.8CaSiO_3$-$0.2Ca_3(PO_4)_2$ eutectic glass-ceramics

D. Sola[a], R. Balda[a,b*], J.I. Peña[c], J. Fernández[a,b]

[a]*Materials Physics Center CSIC-UPV/EHU and Donostia International Physics Center, 20080 San Sebastián, Spain*

[b]*Departamento de Física Aplicada I, Escuela Técnica Superior de Ingeniería, Universidad del Pais Vasco, Alda. Urquijo s/n 48013 Bilbao, Spain*

[c]*Instituto de Ciencia de Materiales de Aragón, Universidad de Zaragoza-CSIC 50018 Zaragoza, Spain*

*wupbacrr@bi.ehu.es

## ABSTRACT

In this work we study the influence of the host matrix on the spectroscopic properties of $Nd^{3+}$ ions in $0.8CaSiO_3$-$0.2Ca_3(PO_4)_2$ eutectic glass and glass-ceramics obtained by the laser floating zone technique at different growth rates in the 100-500 mm/h range. Site-selective emission and excitation spectra of the $^4I_{9/2}\rightarrow{}^4F_{5/2,3/2}$ transitions show the presence of a complex structure which suggests the existence of different crystal field sites for the rare-earth (RE) in these matrices. The spectra of the samples grown at lower rates show more structure and more resolved components. These experimental results suggest that $Nd^{3+}$ ions incorporate in a crystalline phase in these glass-ceramics.

**Keywords:** Rare earth doped materials, Neodymium, laser floating zone, eutectic glass-ceramics.

## 1. INTRODUCTION

The development of optical devices based on lanthanide ion doped materials for their use in telecommunication systems, such as upconversion fibers, optical amplifiers, solid-state lasers, and 3D displays has generated a great deal of interest in the last years [1]. Among the various rare-earth (RE) ions, neodymium has been studied in a variety of glasses due to its potential applications in the field of infrared (IR) optical amplification related with the radiative efficiency of the $^4F_{3/2}\rightarrow{}^4I_{11/2}$ transition. It is well known that the spectroscopic properties of a trivalent rare-earth ion depend on the chemical composition of the glass matrix, which determines the structure and nature of the bonds [2]. For example, spontaneous emission probabilities from levels $^4F_{3/2}$ of $Nd^{3+}$ and $^4I_{13/2}$ of $Er^{3+}$ in oxide glass compositions increase with increasing packing ratio of the glass host [3,4]. The smaller the alkaline or alkaline-earth ions, the larger this packing ratio. Moreover, in silicates, the packing ratio increases with the content of alkali modifier. As an example, referring to the limitations imposed by the former, $SiO_2$ content in silicate glasses ranges typically between 60 and 80 mol% [5]. For lower silica contents the glass tends to undergo devitrification and for higher contents the melt viscosity increases. To overcome these problems, the addition of small amounts of $P_2O_5$ glass former permits to extend the glass forming region in the $CaO$-$SiO_2$-$P_2O_5$ system up to very high modifier concentrations. The limit is close to the $CaSiO_3$-$Ca_3(PO_4)_2$ eutectic formulation where a glass with the highest Ca/(Si+P) ≈1 and Si/P=2 ratios can be produced [6]. This composition corresponds to an inverted glass because the modifier content is larger than the former content, and belongs to the family of the well known bioactive glasses [7]. It was found that the lifetimes and emission cross-sections of the 1.06 μm ($Nd^{3+}$) and 1.5 μm ($Er^{3+}$) emissions in this glass are equivalent to those of the best commercially used alkaline-silicate glasses [8].The fabrication of high quality glasses of this composition is possible by using high solidification and cooling rates, as provided by the laser floating zone (*LFZ*) method. This technique permits

Optical Components and Materials IX, edited by Shibin Jiang, Michel J. F. Digonnet, J. Christopher Dries,
Proc. of SPIE Vol. 8257, 825706 · © 2012 SPIE · CCC code: 0277-786X/12/$18 · doi: 10.1117/12.905649

the control of the solidification rate, providing high axial and radial thermal gradients in the liquid-solid interface, of a paramount importance in the microstructure control, and opens up the possibility of fabricating eutectic glasses and glass-ceramics [8,9]. In this work we study the influence of the processing conditions on the spectroscopic properties of $Nd^{3+}$ in $CaSiO_3$-$Ca_3(PO_4)_2$ eutectic glass-ceramics doped with 1 wt% of $Nd_2O_3$. Site-selective emission and excitation spectra of the $^4I_{9/2} \rightarrow {}^4F_{5/2,3/2}$ transitions have been used to investigate the crystal field changes felt by the $Nd^{3+}$ ion as a consequence of the sample crystallization stage.

## 2. EXPERIMENTAL

### 2.1 Sample fabrication

The precursor rods were obtained from the powder mixture of wollastonite (CS) and tricalcium phosphate (TPC) in the eutectic 80% $CaSiO_3$, 20% $Ca_3(PO_4)_2$ mol% composition. Furthermore, 1 wt% of $Nd_2O_3$ was added to the eutectic composite to obtain the doped samples. The resulting powders were isostatically pressed at 200 MPa for 2 minutes for obtaining ceramic rods which were sintered at 1200ºC for 10 hours.
Glass-ceramic eutectic rods were obtained by the laser floating zone technique, *LFZ*. The laser floating zone system includes a 600 W $CO_2$ semisealed laser (Electronic Engineering Blade 600) emitting at 10.6 μm and an in-house built growth chamber with gold coated metal mirrors for beam focussing and two vertical axes for cylinder displacement. Both axes have independent rotation and translation movements. The mirror system inside the chamber consists of a reflaxicon that transforms the solid beam into a ring that is deflected by a flat mirror at 45º and focused on the ceramic rod by a parabolic mirror producing a homogenous heating; Figure 1. The correct optical alignment is obtained with the aid of a red diode laser coaxial with the infrared beam. Once the precursor is placed in the upper axis, the growth process starts by heating its lower end. When a drop is formed, a small seed placed in the lower axis is approached until a liquid bridge between the precursor and the seed is established. Then the seed is moved away while the precursor is moved towards the molten zone, maintaining constant the volume of the liquid zone. Identical feed and growth rates can be used when equal precursor and eutectic rod diameters are required. To increase or decrease the eutectic rod diameter, the growth rate must be lower or higher respectively than the precursor speed. The precursor and the grown rod are counter rotated to improve the heat distribution in the molten zone. The growth rates were varied between 100 and 500 mm/h in order to modify the crystalline character of the samples. Samples were grown in air, and finally they were annealed at 650ºC for 5 h to relieve inner stresses.

### 2.2 Experimental techniques

The samples temperature was varied between 10 and 300 K in a continuous flow cryostat. Site-selective steady-state emission and excitation spectra were obtained by exciting the sample with a Ti-sapphire ring laser (0.4 $cm^{-1}$ linewidth) in the 770-920 nm spectral range. The fluorescence was analysed with a 0.25 m Triax 190 monochromator, and the signal was detected by a Hamamatsu H10330A-75 photomultiplier and finally amplified by a standard lock-in technique.

## 3. RESULTS AND DISCUSSION

Before considering the spectroscopic properties of $Nd^{3+}$ ions in the glass-ceramics samples, we shall show the results of site-selective spectroscopy for the glass sample. The $^4F_{3/2} \rightarrow {}^4I_{11/2}$ transition of $Nd^{3+}$ ions can show variations in the peak wavelength, linewidth, and spectral profile depending on pumping wavelength due to the site-to-site variation of the local field acting on the ions. Therefore, selective excitation of $Nd^{3+}$ by changing the wavelength of the pump laser provides an additional means of varying the gain profile and affecting the laser operation. To understand these processes it is important to investigate the interaction between monochromatic radiation and an assembly of spectrally inhomogeneous active centers. In order to obtain information about the crystal field site inhomogeneity of $Nd^{3+}$ in these matrices we took advantage of the tunability and narrow bandwidth of the ring Ti-sapphire laser and performed site-selective excitation spectra of the $^4I_{9/2} \rightarrow {}^4F_{5/2,3/2}$ transitions by collecting the luminescence at different wavelengths along the $^4F_{3/2} \rightarrow {}^4I_{11/2}$ transition. As an example, Fig. 2(a) shows the excitation spectra obtained at different emission

wavelengths along the $^4F_{3/2} \rightarrow {}^4I_{11/2}$ transition measured at 10 K. The spectra corresponding to the $^4I_{9/2} \rightarrow {}^4F_{3/2}$ transition show, as expected, two main broad bands associated with the two Stark components of the $^4F_{3/2}$ doublet. However, the low energy component corresponding to the $^4I_{9/2} \rightarrow {}^4F_{3/2}$ doublet narrows and blue-shifts, as the emission wavelength goes from low to high energy. In addition, in the spectrum collected at 1066 nm at least two components are observed. This behavior is a consequence of contributions from $Nd^{3+}$ ions in a multiplicity of environments. The monochromatic radiation excites an isochromat corresponding to a subset of sites, which may not be physically identical. Therefore, the emission line profile is a composition of emissions from two or more statistical site distributions, which may have different natural homogeneous linewidths. The bands corresponding to the $^4I_{9/2} \rightarrow {}^4F_{5/2}$ transition also show a blue shift and a narrowing when the emission wavelength decreases.

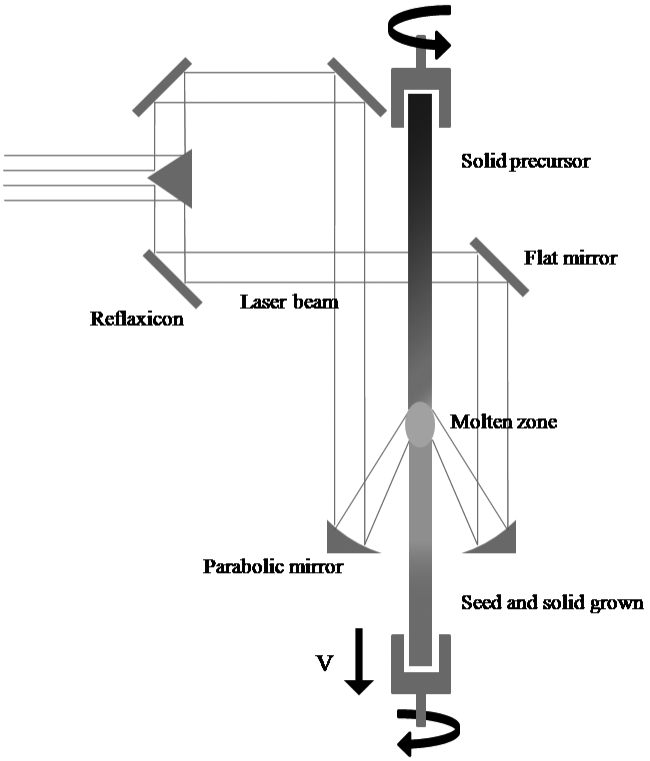


Fig. 1. Sketch of the LFZ system for growing the glass-ceramic samples.

The site-selective steady-state emission spectra of the laser transition were obtained at low temperature for different excitation wavelengths along the $^4I_{9/2} \rightarrow {}^4F_{3/2}$ transition. As can be observed in Fig. 2(b) the shape, peak position, and linewidth of the emission band change as excitation goes from high to low energy. The spectra obtained under excitation at the low energy side of the $^4I_{9/2} \rightarrow {}^4F_{3/2}$ absorption band narrow and red shift. The wavelength of the fluorescence peak shifts from 1059 to 1067 nm by varying the excitation wavelength from 870 to 890 nm whereas the effective linewidth is reduced from about 28 nm to 14 nm.

These results show the rare inhomogeneous behavior of the crystal field felt by $Nd^{3+}$ ions in this glass as well as the relative spectral isolation of the neodymium site distributions that can be excited at a given wavelength. As a consequence, the stimulated emission of $Nd^{3+}$ in this glass shows a tunability of about 10 nm as a function of excitation

wavelength [10]. The presence of this variety of quasi-isolated crystal field site distributions of $Nd^{3+}$ ions in this glass matrix is most probably associated to the glass CaO-modifier rich composition, which allows a broader distribution of $Nd^{3+}$ sites than would be obtained in $SiO_2$-network-forming rich compositions. As can be seen in Fig. 2(b), only when we excite at the high energy side of the low energy component of the $^4I_{9/2} \rightarrow {}^4F_{3/2}$ absorption band it is possible to cover the full spectral range of the $Nd^{3+}$ emission, probably assisted by vibronic transitions.

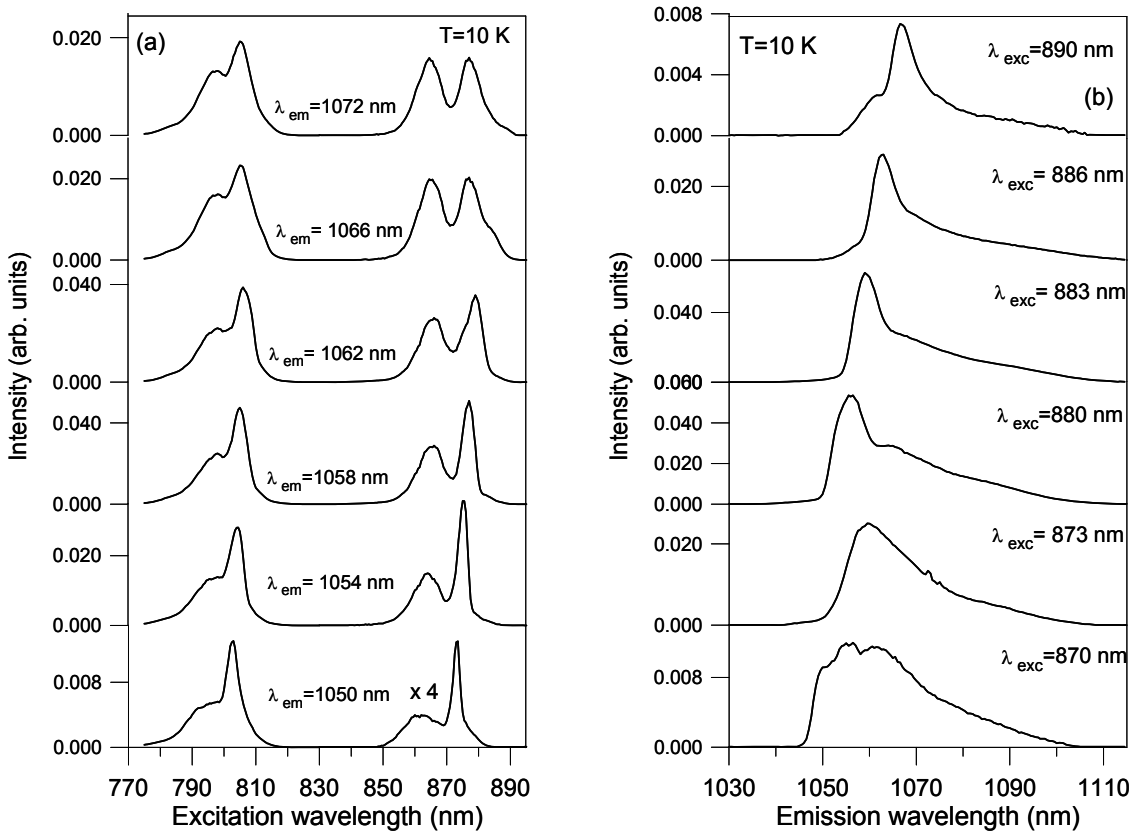


Fig. 2. (a) Excitation spectra of the $^4I_{9/2} \rightarrow {}^4F_{5/2,3/2}$ transitions obtained by collecting the luminescence at different emission wavelengths along the $^4F_{3/2} \rightarrow {}^4I_{11/2}$ emission in the glass sample. The band corresponding to the $^4I_{9/2} \rightarrow {}^4F_{3/2}$ transition has been multiplied by 4 in all cases. (b) Steady-state emission spectra of the $^4F_{3/2} \rightarrow {}^4I_{11/2}$ transition for different excitation wavelengths along the low Stark component of the $^4F_{3/2}$ level.

To study the influence of the processing conditions on the spectroscopic properties of $Nd^{3+}$ ions in the eutectic glass-ceramics we have performed, as in the previous case, site-selective excitation spectra of the $^4I_{9/2} \rightarrow {}^4F_{3/2,5/2}$ transitions collecting the luminescence at different emission wavelengths along the $^4F_{3/2} \rightarrow {}^4I_{11/2}$ transition for the glass-ceramics samples. Figure 3(a) shows the low temperature excitation spectra corresponding to the $^4I_{9/2} \rightarrow {}^4F_{3/2,5/2}$ transitions obtained by collecting the luminescence at 1066 nm for the glass-ceramic samples doped with 1 wt% of $Nd^{3+}$ grown at 100, 250, and 500 mm/h. The spectra corresponding to the $^4I_{9/2} \rightarrow {}^4F_{3/2}$ transition show at least four main bands instead of the two bands associated with the two Stark components of the $^4F_{3/2}$ doublet in a low crystal field symmetry, which indicates the presence of different environments for $Nd^{3+}$ ions in these matrices. By comparing these with the excitation spectra of the glass sample obtained by collecting the luminescence at 1066 nm, the spectra of this transition in the glass-ceramic samples show two new peaks at around 859 and 886 nm, being their position almost independent of the growth rate. The spectra corresponding to the $^4I_{9/2} \rightarrow {}^4F_{5/2}$ transition also show a new sharp peak at around 810 nm, not

observed in the excitation spectra of the glass sample, which indicates that $Nd^{3+}$ ions are in a crystalline environment. Moreover, the spectra show more structure for the sample grown at 100 mm/h which corresponds to a more crystalline character. These experimental results suggest that $Nd^{3+}$ ions incorporate in a crystalline phase in these glass-ceramics.

Once the behaviour of the excitation spectra had been studied as a function of the growth rate, the site-selective steady-state emission spectra of the laser transition were obtained at low temperature for different excitation wavelengths along the $^4I_{9/2}\rightarrow{}^4F_{3/2}$ absorption band for the three glass-ceramic samples. As an example, Fig. 3(b) shows the low temperature emission spectra corresponding to the $^4F_{3/2}\rightarrow{}^4I_{11/2}$ transition obtained by exciting at different wavelengths along the $^4I_{9/2}\rightarrow{}^4F_{3/2}$ transition for the sample obtained with a growth rate of 100 mm/h and doped with 1wt% of $Nd_2O_3$. As can be seen, different emission spectra are obtained depending on the excitation wavelength. The spectrum obtained under excitation at the low energy peak of the $^4I_{9/2}\rightarrow{}^4F_{3/2}$ absorption band at 886.5 shows a narrow line with an effective linewidth of 3.1 nm centered at around 1067 nm together with other Stark components, which suggests that at this wavelength $Nd^{3+}$ ions in a crystalline phase are excited. The spectra obtained at 857, 865, and 875 nm show a complex behavior with different positions for the Stark components probably due to the superposition of the emission from $Nd^{3+}$ ions in different environments. The spectra are similar for the samples grown at 250 and 500 mm/h whereas less resolved spectra appear for the sample grown at 500 mm/h.

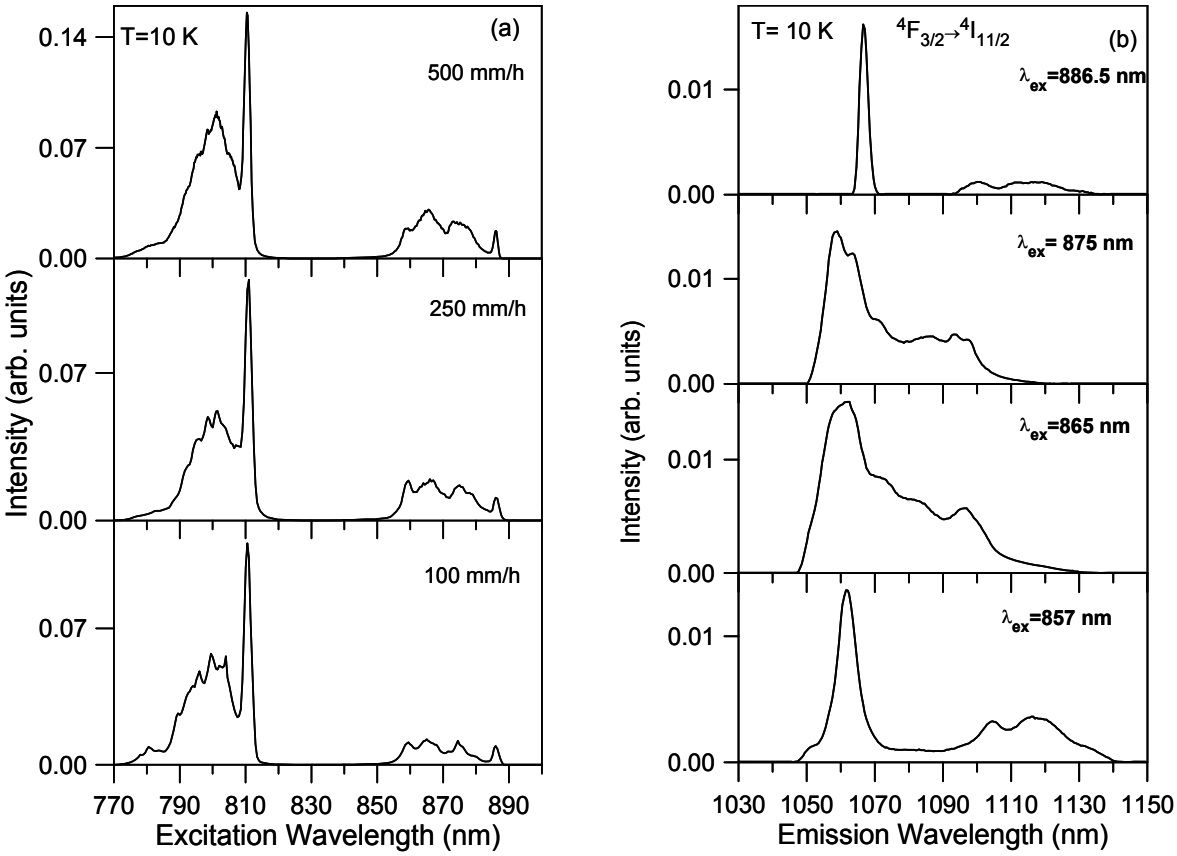


Fig. 3. (a) Excitation spectra of the $^4I_{9/2}\rightarrow{}^4F_{5/2,3/2}$ transitions obtained by collecting the luminescence at different emission wavelengths along the $^4F_{3/2}\rightarrow{}^4I_{11/2}$ emission for the glass-ceramic samples grown at 100, 250, and 500 mm/h. (b) Steady-state emission spectra of the $^4F_{3/2}\rightarrow{}^4I_{11/2}$ transition for different excitation wavelengths along the $^4I_{9/2}\rightarrow{}^4F_{3/2}$ transition for the sample grown at 100 mm/h.

## SUMMARY

Glass-ceramic eutectic rods of composition $0.8CaSiO_3$-$0.2Ca_3(PO_4)_2$ doped with 1 wt% of $Nd_2O_3$ have been obtained by the laser floating zone technique at different growth rates between 100 and 500 mm/h. The low temperature spectroscopic properties of $Nd^{3+}$ ions have been investigated and compared with those found in the glass sample.

The spectral shift and narrowing observed in the steady-state emission spectra of the $^4F_{3/2}\rightarrow{}^4I_{11/2}$ transition under selective excitation along the $^4I_{9/2}\rightarrow{}^4F_{3/2}$ absorption band, reveal the existence of a huge variety of spectrally isolated distributions of $Nd^{3+}$ sites in the glass sample.

In addition to the broad bands observed in the glass matrix, the excitation spectra of the glass-ceramic samples show sharp peaks indicating a crystalline environment for $Nd^{3+}$ ions. The spectra of the samples grown at lower rates show more structure and more resolved components. Furthermore, the emission spectra measured at different excitation wavelengths along the $^4I_{9/2}\rightarrow{}^4F_{3/2}$ band show the existence of different environments for $Nd^{3+}$ ions. These results suggest that $Nd^{3+}$ ions incorporate in a crystalline phase in these glass-ceramics. Further experiments are in progress to correlate the spectroscopic properties with the microstructure of these eutectics.

## ACKNOWLEDGMENTS

This work was supported by the Spanish Government MEC under Projects No. MAT2009-14282-C02-02, FIS2011-27968, Consolider SAUUL CSD2007-00013, and Basque Country Government (IT-331-07). Daniel Sola thanks the JAE-DOC program and the Science and Technology Inter-Ministry commission of Spain and FEDER founds of the EC under project MAT2009-13979-C03-03 for the financial support of his contract.

## REFERENCES

[1] Downing E., Hesselink L., Ralson J., Macfarlane R., "A Three-Color, Solid-State, Three-Dimensional Display", *Science* **273**, 1185-1189, (1996).
[2] Weber M.J., "Science and technology of laser glass", *J. Non-Cryst. Solids* **123**, 208-222, (1990).
[3] Takebe H., Nageno Y., Morinaga K., "Compositional Dependence of Judd-Ofelt Parameters in Silicate, Borate, and Phosphate Glasses" , *J. Am. Ceram. Soc*. **78**, 1161-1168, (1995).
[4] Takebe H., Morinaga K., Izumitani T., "Correlation between radiative transition probabilities of rare-earth ions and composition in oxide glasses" , *J. Non-Cryst. Solids* **178**, 58-63, (1994).
[5] Righini G.C., Pelli S., Brenci M., Ferrari M., Duverger C., Montagna M., Dall'Igna R., "Active optical waveguides on Er and Er/Yb-doped silicate glasses", *J. Non-Cryst. Solids* **284,** 223-229, (2001).
[6] De Aza P.N., Guitian F., De Aza S., "Phase diagram of wollastonite-tricalcium phosphate" , *J. Am. Ceram. Soc.* **78**, 1653-1656, (1995).
[7] Hench L.L., "Bioceramics: From Concept to Clinic", *J. Am. Ceram. Soc.*, 74, 1487-1510, (1991).
[8] Pardo J.A., Peña J.I., Merino R.I., Cases R., Larrea A., Orera V.M., "Spectroscopic properties of $Er^{3+}$ and $Nd^{3+}$ doped glasses with the $0.8CaSiO_3$–$0.2Ca_3(PO_4)_2$ eutectic composition", *J. Non-Cryst. Solids* **298**, 23-31, (2002).
[9] Llorca J., Orera V.M., "Directionally solidified eutectic ceramic oxides", *Prog. Mater. Sci*. **51**, 711-809, (2006).
[10] Balda Rolindes, Fernández Joaquín, Iparraguirre Ignacio, Azkargorta Jon, García-Revilla Sara, Peña Jose Ignacio, Merino Rosa I., Orera Víctor M., "Broadband laser tunability of $Nd^{3+}$ ions in $0.8CaSiO_3$-$0.2Ca_3(PO_4)_2$ eutectic glass", *Opt. Express* 17, 4382-4387, (2009).